Annals of Physics 326 (2011) 2845–2867

Contents lists available at SciVerse ScienceDirect

Annals of Physics

journal homepage: www.elsevier.com/locate/aop

Nonclassical effects in a highly nonlinear generalized homogeneous Dicke model

Horacio Grinberg*,[1]

Department of Physics, Facultad de Ciencias Exactas y Naturales, University of Buenos Aires, Pabellón 1, Ciudad Universitaria, (1428) Buenos Aires, Argentina
IFIBA, Consejo Nacional de Investigaciones Científicas y Técnicas, Argentina

ARTICLE INFO

Article history:
Received 17 February 2011
Accepted 30 July 2011
Available online 25 August 2011

Keywords:
Dicke model
Rotating wave approximation
Normal squeezing
Variance squeezing
Linear entropy
Entanglement

ABSTRACT

An intensity dependent nonlinear coupling model of N two-level atoms (generalized Dicke model) interacting dispersively with a bimodal cavity field via two-photon transitions is investigated in a scenario where the rotating wave approximation is assumed. The model becomes homogeneous in the sense that the spin transition frequency is the same for all atoms and the coupling constants emerging from the collective interactions of the atomic system with the cavity field depend only on the particular radiation field mode. This allows us to represent the Dicke Hamiltonian entirely in terms of the total angular momentum J. It is assumed that, initially, the atomic system and the field are in a disentangled state where the field modes are in Glauber coherent states and the atomic system is a superposition of states $|JM\rangle$ (Dicke states). The model is numerically tested against simulations of normal squeezing variance of the field, squeezing factors based on the Heisenberg uncertainty principle, along with the statistical properties of the light leading to the possible production of nonclassical effects, such as degree of second-order coherence in the modes, degree of intermode correlation, as well as violation of the Cauchy–Schwartz inequality. Analytical expression of the total density operator matrix elements at $t > 0$ shows the present nonlinear model to be strongly entangled, which is reflected in the time evolution of the linear entropy, where the superposition states are reduced to statistical mixtures. Thus, the present generalized

* Correspondence to: Departamento de Física, Facultad de Ciencias Exactas y Naturales, Universidad de Buenos Aires, Pabellón 1, Ciudad Universitaria, (1428) Buenos Aires, Argentina. Tel.: +54 11 4576 3353; fax: +54 11 4576 3357.
E-mail address: grinberg@df.uba.ar.

[1] Under Contract, Consejo Nacional de Investigaciones Científicas y Técnicas (CONICET), Argentina.

0003-4916/$ – see front matter
doi:10.1016/j.aop.2011.07.010

Dicke model does not preserve the modulus of the Bloch vector. The computations, performed in the weak coupling and strong field limits, were conducted via second-order Dyson perturbative expansion of the time evolution operator matrix elements for the totality of the angular momentum states of the atomic system.

1. Introduction

The Dicke model [1] describes the collective behavior of an ensemble two-level atoms coupling, via dipole interaction, with a cavity field of dimension less than the radiation wavelength. It has attracted considerable attention recently, mainly due to the fact that the Dicke model is closely related to many interesting fields in quantum optics, such as coupled arrays of optical cavities used to simulate the behavior of strongly correlated systems [2–4], superconducting charge qubits [5], and the superrradiant behavior by an ensemble of quantum dots [6]. These studies were motivated by the pioneering work on cooperative spontaneous emission made by Dicke [1] who realized that radiation from N identical two-level systems (spins 1/2) cannot be treated as a sum of N independent radiative processes but rather as a collective quantum phenomenon that involves all N spins and a photon mode even on the level of perturbation theory.

When the Dicke system is driven by a single mode external laser field in the strong field limit $\overline{n} \gg N$, where $\overline{n}$ is the mean photon number in the initial state, it shows strong atom–atom correlations giving rise to nonclassical behavior of the emitted radiation field [7,8]. Apart from the standard Dicke model many generalized Dicke models have also been proposed and studied [9–19]. Generally, they all display a rich dynamics, with many interesting nonclassical features [20–23] that manifest themselves in the clearest way when the cavity field is prepared in the coherent state [24].

Among the various phenomena associated to the generation of nonclassical effects emerging from the dynamics of the Dicke model, the quantum entanglement has been recently investigated in detail [25–29]. In fact, it arises when a superposition principle is applied to composite systems. After two quantum particles have interacted, they can no longer be described independently of each other. Their "entangled" state is not a tensor product of eigenstates of observables pertaining to the two particles, which would describe independent systems with well-defined properties. It is instead a superposition of such products. The state of one particle is determined by a measurement performed on the other. Moreover, the same entangled state can be written in different forms, corresponding to different sets of noncommuting observables for the two particles. These quantum correlations are independent of the particles' spatial separation and introduce a fundamental nonlocal aspect in the quantum world. Beyond these fundamental aspects, entangled states might have important applications for information transmission or processing, e.g. elements of binary information can be coded in two-state quantum systems called qubits.

Squeezing, which redistributes quantum fluctuations between two noncommuting observables while preserving the minimum uncertainty product, has also been extensively studied in boson systems [8,30]. The quantum mechanical correlations between photons, established through nonlinear interactions, play an essential role in the generation of squeezed states of light.

Besides the importance in the study of fundamentals of quantum theory, the realization of the Dicke model plays a crucial role in quantum information technology and quantum communication. Indeed, arrays of atoms (qubits) are ideal candidates for quantum registers and their controlled interaction with photons allows us to realize atom–light quantum interfaces [31] and to distribute entanglement to different nodes of quantum networks. As is well-known, pumping multiatom ($N \gg 1$) samples with externally applied coherent fields can induce sensitive atomic responses due to the collective interactions of atoms with the environmental electromagnetic field [7].

Spin or angular momentum systems have often been regarded as squeezed if the uncertainty of one spin component, say $\langle \Delta J_x^2 \rangle$ or $\langle \Delta J_y^2 \rangle$ is smaller than $\frac{1}{2}|\langle J_z \rangle|$. This definition implies that a *coherent spin state* (CSS) is already squeezed if it is placed in an appropriate system of coordinates, and also that spin can be squeezed by just rotating the CSS. This subject has been vigorously studied [32–35]

due to its close connection to quantum entanglement, the main ingredient for quantum information in general. More generally, the spin squeezed states can be a source of entanglement in an ensemble of large number of atoms. Thus, spin squeezing is possible in optical systems which are inherently nonlinear.

For certain variants of the Dicke Hamiltonian, incorporation of two laser fields with different amplitudes and frequencies in the quantum regime involving two-photon transitions resists exact analytical solution, even in the case of exact simultaneous resonance of the N two-level atoms with both modes of the cavity field. A systematic analysis concerning the nondegenerate two-mode nonclassical states associated with off-resonant states of the cavity field coupled with an ensemble of N two-level atoms is not completely documented so far, and this motivates us to introduce in this paper a generalized Dicke model in which two-photon transitions are mediated by two modes of photons in off-resonant states. The transient dynamics of such generalized model is an important issue in view of the possibility of observing a variety of typical nonlinear phenomena, such as entanglement propagation through the whole atomic system and entangled light via nonlinear vacuum–multiparticle interactions.

In off-resonant states the interaction picture Hamiltonian of the Dicke model becomes time-dependent. Moreover, since in this case the set of interaction picture Hamiltonians $\mathcal{V}(t_1)$, $\mathcal{V}(t_2)$, ..., taken at different times $t_1, t_2, \ldots$ fail to commute, Dyson perturbation expansion of the time evolution operator matrix elements truncated to a finite order constitutes the ideal tool to deal with this many-body problem [36,37].

The objective of the present study is to develop a generalized homogeneous Dicke model in which an intensity dependent nonlinear coupling interacting dispersively with a bimodal cavity field via two-photon transitions is incorporated in a scenario where the rotating wave approximation (RWA) is assumed. The system dynamics will be explored through the density operator formalism, assuming that, initially, the atomic system and the field are in a disentangled state, the field modes are in Glauber coherent states, and the atomic system is prepared in a superposition of angular momentum states $|JM\rangle$ with the initial coherent state of the field given by a Poisson distribution. In particular, analytical expression of the total density matrix elements at $t > 0$ reveals that the present nonlinear model is strongly entangled, which is reflected in the time evolution of the linear entropy. The incorporation of an ensemble of angular momentum states $|JM\rangle$ represents a novel feature of the present treatment which helps to understand certain collective effects related to the photon-distribution mechanism when different specific initial atomic states are used [8].

The present model, emerging from the solution of the time-dependent Schrödinger equation via second-order Dyson perturbation expansion of the chronologically ordered time-dependent evolution operator, is numerically tested against numerical simulations of normal squeezing variance of the field, squeezing factors based on the Heisenberg uncertainty principle, and entanglement as measured by the linear entropy. It is clearly observed, for example, that during the time evolution of the linear entropy the superposition states are reduced to statistical mixtures. Thus, the present generalized Dicke model does not preserve the modulus of the Bloch vector. Under certain conditions angular momentum superposition states may exhibit other nonclassical effects, such as photon antibunching, sub-Poissonian photon statistics and violation of the Cauchy–Schwartz inequality. Thus, the statistical properties of the light such as degree of second-order coherence in the modes, degree of intermode correlation, and possible violation of the Cauchy–Schwartz inequality will also be explored.

This article is organized accordingly as follows. In Section 2, the Hamiltonian of the homogeneous Dicke model under the RWA is described in detail. The coherent atomic states (Bloch states) obtained by the rotation of the angular momentum ground state, and radiation field Glauber states which comprise both the initial state wavefunction are given and the interaction picture representation of the generalized Dicke model is introduced and discussed. This allows us to obtain the time-dependent density operator matrix elements, from which the dynamical behavior of the whole system can be analyzed, even during short periods of time at the very beginning of the time evolution. Section 3 is devoted to a brief discussion of the numerical simulations. A summary and some concluding remarks are finally given in Section 4. The article is complemented with two appendices. In Appendix A, the radiation field matrix elements in the Fock space are listed along with some formulas necessary to compute the antibunching effect, sub-Poissonian statistics of the field, and violation of

the Cauchy–Schwartz inequality. In Appendix B, a set of rotated operators on the Bloch sphere are obtained via total (atomic system plus field) density operator matrix elements valid to all orders.

2. Atom–cavity interaction in the generalized Dicke model

Let us consider a bosonic system S, with Hilbert space $\mathcal{H}^{(S)}$ which is coupled with an ensemble of N two-level atoms, with Hilbert space $\mathcal{H}^{(B)}$. Let us assume that the complete system is in thermal equilibrium with a reservoir at temperature β^{-1}. It is important to keep in mind that the presence of the reservoir only takes the N two-level atoms and the bosonic modes in thermal equilibrium. Let us denote by $\mathcal{H}_S$, $\mathcal{H}_B$, and $\mathcal{H}_I$ the Hamiltonians of the bosonic field, the N two-level atoms, and the interaction between both systems, respectively. The Hamiltonian for the total system can be written as

$$\mathcal{H} = \mathcal{H}_S \otimes I_B + I_S \otimes \mathcal{H}_B + \mathcal{H}_I \equiv \mathcal{H}_0 + \mathcal{H}_I, \tag{1}$$

where I_S and I_B denote the identities in the Hilbert spaces of the bosonic field and the ensemble of N atoms.

The aim of this section is to introduce the necessary formalism to develop generalized models of N two-level systems (qubits) interacting dispersively with a cavity in which the validity of the RWA is assumed. In this scenario, we consider a generalized version of Dicke model that describes a collection of N two-level atoms interacting with a two-mode radiation field and induces two-photon transitions. Furthermore, an intensity dependent nonlinear coupling is explicitly incorporated in the Hamiltonian. This makes the present model to be highly nonlinear and therefore only approximate solutions can be developed. The system dynamics will be explored through the density operator formalism emerging from the chronologically ordered time-dependent perturbation Dyson expansion of the evolution operator matrix elements. We consider the situation where the linear dimension of the total atomic system is small compared to the correlation length of the reservoir; therefore, the N atoms interact collectively with the reservoir. We can further proceed by assuming that for a fixed mode j of the reservoir all the coupling constants G_{ij}, $i = 1, 2, \ldots, N$, are equal, i.e., $G_{ij} \equiv G_j$. We will ignore the interaction between the atoms (qubits) and treat the atomic system as a large spin ($N = 2J$).

Assuming that the frequency ν_j of one of the cavity modes is near resonant with the (constant) energy gap ω of the two-level atoms, such a situation generates a homogeneous physical model in which the two-level atoms effectively interact only with that mode, and the other bosonic mode does not couple with the two-level atoms. Under these circumstances the model is reduced to a single mode of the bosonic field with the photon operators interacting with an ensemble of atoms. This rather simplified situation will not be considered in this paper, as it was extensively investigated over the past decade. Instead, we will consider the much more complex homogeneous model involving intensity dependent photon operators along with two modes of the cavity, i.e., we will assume a nonzero detuning for each mode involving off-resonant states (this corresponds obviously to the nondegenerate case of the two modes of the field). The resulting complete Hamiltonian under the RWA for such model reads ($\hbar = 1$)

$$\mathcal{H} = \sum_{j=1}^{2} \nu_j a_j^\dagger a_j \otimes I_B + \omega I_S \otimes J_z + \sum_{j=1}^{2} \frac{G_j}{\sqrt{N}} (J_+ \otimes R_j^k + J_- \otimes R_j^{\dagger k}), \tag{2}$$

where the first two terms and the last term on the rhs correspond to $\mathcal{H}_0$ and $\mathcal{H}_I$, respectively. ν_j and G_j are the photon frequency and atom–field coupling constant (vacuum Rabi frequency) for the mode j; $a_j^\dagger$ (a_j) is the canonical creation (annihilation) bosonic operator for the mode j, the zero-point energy of the bosonic field was omitted, and a constant term $1/2(\omega_a + \omega_b)$, where ω_a and ω_b are the energies of the ground ($|a\rangle$) and excited ($|b\rangle$) states of the two-level many-atom system, was ignored. The two-level many-atom operators $J_z, J_\pm$ are the usual angular momentum operators for a pseudospin of length $J = N/2$ (collective modes associated to the atomic pseudospin operators) which satisfy the standard angular momentum commutation relations $[J_z, J_\pm] = \pm J_\pm$, along with the angular-momentum-like commutation relations $J \times J - iJ = 0$ corresponding to a $2J + 1$-dimensional space of

angular momentum J and therefore they constitute a basis of the Lie $SO(3)$ algebra. These collective Pauli mode spin operators are constructed by single-atomic operators $\{\sigma_+^\alpha, \sigma_-^\alpha, \sigma_z^\alpha; \alpha = 1, \ldots, N\}$ which are kinematically independent and obey the usual $SU(2)$ commutation relations. Thus, these atom-flip operators characterize an effective single two-level atom with transition frequency $\omega = \omega_b - \omega_a$. Note that inhomogeneities in G_{ij} and/or ω_j would have forbidden to represent the Hamiltonian in Eq. (2) in terms of the total angular momentum J. In Eq. (2), the radiation field operators R_j^k and $R_j^{\dagger k}$ are intensity dependent *shifting* operators involving k photons, i.e.,

$$R_j^k = a_j^k (a_j^\dagger a_j)^{1/2}, \tag{3}$$

and its hermitian conjugate

$$R_j^{\dagger k} = (a_j^\dagger a_j)^{1/2} a_j^{\dagger k}. \tag{4}$$

A simplified model is achieved if we assume that the N two-level atoms and the bosonic modes are in the interior of a high-Q lossless cavity.

2.1. Coherent atomic states and Glauber states: initial state wavefunction

The Hilbert space of the collective atomic operators is spanned by the Dicke states, which are simply the usual angular momentum states $|JM\rangle$ $(M = -J, -J+1, \ldots, J)$ obtained as the simultaneous eigenstates of the $SU(2)$ Casimir operators J^2 and $J_z = 1/2[J_+, J_-]$. They are given by [38]

$$|JM\rangle = \frac{1}{(M+J)!}\left(\frac{2J}{M+J}\right)^{-1/2} J_+^{M+J}|J-J\rangle, \tag{5}$$

with eigenvalue M and where the ground state $|J-J\rangle$ is defined by $J_-|J-J\rangle = 0$. Let us consider the rotation operator $R_{\theta,\phi}$ which produces a rotation through an angle θ about an axis $\hat{n} = (\sin\phi, -\cos\phi, 0)$

$$R_{\theta,\phi} = e^{-i\theta J_n} = e^{-i\theta(J_x \sin\phi - J_y \cos\phi)} = e^{\zeta J_+ - \zeta^* J_-}, \tag{6}$$

where

$$\zeta = \frac{1}{2}\theta e^{-i\phi} \quad (0 \le \theta \le \pi; 0 \le \phi \le 2\pi). \tag{7}$$

A coherent atomic state, or Bloch state, $|\theta, \phi\rangle$ is obtained by rotation of the ground state $|J-J\rangle$, i.e.,

$$|\theta, \phi\rangle \equiv R_{\theta,\phi}|J-J\rangle, \tag{8}$$

which is the group definition of the atomic coherent states. The Bloch states $|\theta, \phi\rangle$ satisfy a completeness relation given by

$$(2J+1)\int |\theta, \phi\rangle \frac{d\Omega}{4\pi} \langle\theta, \phi| = 1, \tag{9}$$

where $d\Omega = \sin\theta\, d\theta\, d\phi$ is the solid-angle volume element at (θ, ϕ) on S^2 (Bloch sphere). The Bloch sphere is a well-known tool in quantum optics, where the simple qubit state is faithfully represented, up to an overall phase factor, by a point on a standard sphere with radius unity, whose coordinates are expectation values of the atomic set operators of the system.

Using the disentangling theorem for angular momentum operators [39], the rotation $R_{\theta,\phi}$ given by Eq. (6) becomes

$$R_{\theta,\phi} = e^{-\tau^* J_-} e^{-\ln(1+|\tau|^2) J_z} e^{\tau J_+} = e^{\tau J_+} e^{\ln(1+|\tau|^2) J_z} e^{-\tau^* J_-}, \tag{10}$$

where

$$\tau = e^{-i\phi} \tan\frac{1}{2}\theta, \tag{11}$$

defines the stereographic projection from the south pole of the sphere to the plane passing through the equator, with complex coordinates τ, τ^*.

The last form of Eq. (10) which we call the normally ordered form, immediately gives the expansion of $|\theta, \phi\rangle$ in terms of Dicke states

$$|\tau\rangle \equiv |\theta, \phi\rangle = R_{\theta,\phi}|J - J\rangle = \left(\frac{1}{1 + |\tau|^2}\right)^J e^{\tau J_+}|J - J\rangle, \tag{12}$$

whence, expanding the exponential and using Eq. (5)

$$\begin{aligned}\langle JM \mid \theta, \phi\rangle &= \binom{2J}{M+J}^{1/2} \frac{\tau^{M+J}}{[1 + |\tau|^2]^J} \\ &= \binom{2J}{M+J}^{1/2} \sin^{J+M}\left(\frac{1}{2}\theta\right) \cos^{J-M}\left(\frac{1}{2}\theta\right) e^{-i(J+M)\phi}.\end{aligned} \tag{13}$$

These coherent states are non-orthogonal, with

$$\langle \tau_1 \mid \tau_2\rangle = \frac{(1 + \tau_1^*\tau_2)^{2J}}{(1 + |\tau_1|^2)^J (1 + |\tau_2|^2)^J}. \tag{14}$$

In particular, $\langle \tau|\tau\rangle = 1$. In this model the initial state vector involving two modes of the field is represented by

$$|Z\tau\rangle \equiv |Z\rangle \otimes |\tau\rangle = |z_1 z_2\rangle \otimes |\theta, \phi\rangle, \tag{15}$$

i.e., the direct product of a field canonical coherent state $|Z\rangle$ and a pseudospin coherent state $|\tau\rangle \equiv |\theta, \phi\rangle$. Thus, while $|Z\rangle$ is defined in the 'particle' Hilbert space, $|\tau\rangle$ is defined in the $(2J+1)$-dimensional space. The coherent states (Glauber states) $|z_j\rangle$ are given by $(j = 1, 2)$

$$|z_j\rangle = \exp\left(z_j a_j^\dagger - \frac{1}{2}|z_j|^2\right)|0\rangle_j, \tag{16}$$

where the z_j are complex numbers and $|0\rangle_j$ is the bosonic oscillator vacuum state for the j-mode. These coherent states are non-orthogonal

$$\langle z_1 \mid z_2\rangle = \exp(-|z_1|^2/2 + z_1^* z_2 - |z_2|^2/2), \tag{17}$$

and satisfy the closure relation

$$\int |z_j\rangle \frac{d^2 z_j}{\pi} \langle z_j| = 1_j, \tag{18}$$

with 1_j the unit operator for the j-mode and the overlap $\langle n_1 n_2|z_1 z_2\rangle$ given by a Poisson distribution

$$\langle n_1 n_2 \mid z_1 z_2\rangle = \langle n_1 \mid z_1\rangle \langle n_2 \mid z_2\rangle, \tag{19}$$

with

$$|\langle n_j \mid z_j\rangle|^2 = \exp(-|z_j|^2) \frac{|z_j|^{2n_j}}{n_j!}. \tag{20}$$

The dynamics of the present model is not stationary and depends on the initial conditions of the system and the cavity field. Thus, it is assumed that, initially, the field modes are in coherent states $|z_1 z_2\rangle$ and the atomic system is a superposition of states $|JM\rangle$, that is, the atomic system and the field are initially in a disentangled state with density operator

$$\rho(0) = \rho^f(0) \otimes \rho^S(0) = |\psi(0)\rangle\langle\psi(0)|, \tag{21}$$

where $\rho^f(0)$ and $\rho^S(0)$ are density operators at $t = 0$ of the field and the atomic ensemble respectively, and

$$|\psi(0)\rangle = \sum_{M=-J}^{J} \sum_{n_1=0}^{\infty} \sum_{n_2=0}^{\infty} C_M(0) C_{n_1 n_2}(0) |JM\rangle \otimes |n_1 n_2\rangle, \tag{22}$$

with coefficients $C_M(0) \equiv \langle JM|\theta, \phi\rangle$, $C_{n_1 n_2}(0) \equiv \langle n_1 n_2|z_1 z_2\rangle$. It is further assumed that at $t = 0$, the two modes have the same photon distribution, i.e., the density operator of the field is written as

$$\rho^f(0) = \sum_{n_1=0}^{\infty} \sum_{n_2=0}^{\infty} \sum_{m_1=0}^{\infty} \sum_{m_2=0}^{\infty} C_{n_1}(0) C_{n_2}(0) C^*_{m_1}(0) C^*_{m_2}(0) \mathcal{P}^{n_1 m_1}_{n_2 m_2}, \tag{23}$$

where $\mathcal{P}^{n_1 m_1}_{n_2 m_2} = |m_1 m_2\rangle\langle n_1 n_2|$ is the two-mode Fock space projection operator. Thus, we write

$$C_{m_1 m_2}(0) = [\rho^f_{m_1 m_1}(0) \rho^f_{m_2 m_2}(0)]^{1/2}, \tag{24}$$

while the density operator of the $2N$-level atomic system is given by

$$\rho^S(0) = \sum_{M=-J}^{J} \sum_{M'=-J}^{J} C_M(0) C^*_{M'}(0) \mathcal{P}^{JM}_{JM'}, \tag{25}$$

where $\mathcal{P}^{JM}_{JM'} = |JM\rangle\langle JM'|$ is the projection operator in the angular momentum space.

It is well known that the quantum coherences which are built up during the interaction process significantly affect the dynamics of the atomic system. Thus, in order to investigate the nonclassical behavior of the present model we introduce in the next Subsection the interaction picture representation of this generalized Dicke model.

2.2. Interaction picture representation of the generalized Dicke model

Introducing the unitary time evolution operator for the unperturbed Hamiltonian

$$\mathcal{U}_0(t) = \exp(-i\mathcal{H}_0 t), \tag{26}$$

which merely contributes a phase factor in each atomic subspace, the interaction picture Hamiltonian is given by

$$\mathcal{V}(t) = \mathcal{U}_0^\dagger(t) \mathcal{H}_I \mathcal{U}_0(t), \tag{27}$$

where H_I is given by the last term on the rhs of Eq. (2). Using the Baker–Campbell–Hausdorff expansion

$$\exp(\alpha A)\, B\, \exp(-\alpha A) = B + \alpha[A, B] + \alpha^2/2!\, [A, [A, B]] + \ldots, \tag{28}$$

along with the commutation relations

$$[a_j^\dagger a_j, R_i^k] = -k R_i^k \delta_{ij}, \tag{29}$$

$$[a_j^\dagger a_j, R_i^{\dagger k}] = k R_i^{\dagger k} \delta_{ij}, \tag{30}$$

and consequently noting that

$$e^{i\nu_j a_j^\dagger a_j t} R_j^k e^{-i\nu_j a_j^\dagger a_j t} = R_j^k e^{-i\nu_j k t}, \tag{31}$$

$$e^{i\nu_j a_j^\dagger a_j t} R_j^{\dagger k} e^{-i\nu_j a_j^\dagger a_j t} = R_j^{\dagger k} e^{i\nu_j k t}, \tag{32}$$

and

$$e^{i\omega t J_z} J_+ e^{-i\omega t J_z} = J_+ e^{i\omega t}, \tag{33}$$

the interaction picture Hamiltonian in Eq. (27) can be written as

$$\mathcal{V}(t) \equiv \mathcal{V}_1(t) + \mathcal{V}_2(t) = \sum_{j=1}^{2} \frac{G_j}{\sqrt{N}} (J_+ \otimes R_j^k e^{i\Delta_j t} + h.c.), \tag{34}$$

with the detuning parameter Δ_j for the mode j given by

$$\Delta_j = \omega - k v_j. \tag{35}$$

These detunings between the cavity mode and the atomic transition can have an important influence on the nonclassical effects, as recently reported in the case of a two-level atom coupled to a single mode of cavity fields [40].

To proceed further it is observed from Eq. (34) that

$$[\mathcal{V}_1(t), \mathcal{V}_2(t)] = \frac{G_1 G_2}{J} J_z \otimes (R_1^k R_2^{\dagger k} e^{i(\Delta_1 - \Delta_2)t} - h.c.). \tag{36}$$

Thus, the nonvanishing of this commutator requires special care. Moreover, since in this model system $\mathcal{H}_0$ does not commute with $\mathcal{H}_I$, the set of interaction picture Hamiltonians $\mathcal{V}(t_1)$, $\mathcal{V}(t_2)$, ..., taken at different times $t_1, t_2, \ldots$, fail to commute. In fact, after some rather lengthy algebra, the commutator $[\mathcal{H}(t_1), \mathcal{H}(t_2)]$ is found to be

$$\begin{aligned}[\mathcal{V}(t_1), \mathcal{V}(t_2)] &= \sum_{i=1}^{2}\sum_{j=1}^{2}[\mathcal{V}_i(t_1), \mathcal{V}_j(t_2)] \\ &= \left[i \sum_{j=1}^{2} \frac{G_j^2}{J} (J_+ J_- \otimes [R_j^k, R_j^{\dagger k}] + 2 J_z \otimes R_j^{\dagger k} R_j^k) \sin[\Delta_j (t_1 - t_2)] \right. \\ &\quad \left. + \frac{G_1 G_2}{J} J_z \otimes (R_1^k R_2^{\dagger k} (e^{i(\Delta_1 t_1 - \Delta_2 t_2)} - e^{i(\Delta_1 t_2 - \Delta_2 t_1)}) - h.c.) \right],\end{aligned} \tag{37}$$

which clearly does not vanish, except in the (nontrivial) particular case of exact simultaneous resonance of both modes with the spin transition frequency. In the present paper, we assume that the boson modes are not tuned in resonance with the spins ω. If the boson modes are strongly detuned ($|\omega - k v_j| \gg \langle G_j^2 \rangle^{1/2}$) the interaction between them is weak and the model can be analyzed perturbatively. To this end, perturbation expansion of the time evolution operator matrix elements truncated to a finite order will be used. This time evolution operator in the interaction picture representation reads (Dyson expansion)

$$U_I(t) = \mathcal{F} \exp\left[-i \int_0^t \mathcal{V}(t) dt \right], \tag{38}$$

where $\mathcal{F}$ is the time-ordering chronological operator, which is a shorthand notation for the expansion

$$\begin{aligned}\mathcal{F} \exp\left[-i \int_0^t \mathcal{V}(t) dt \right] &= 1 - i \int_0^t \mathcal{V}(t_1) dt_1 \\ &\quad + (-i)^2 \int_0^t dt_1 \int_0^{t_1} dt_2 \mathcal{V}(t_1)\mathcal{V}(t_2) + \cdots \equiv \sum_{n=0}^{\infty} U_{In}(t).\end{aligned} \tag{39}$$

The entangled interaction picture state vector at any time t emerges from the coherent state $|\psi(0)\rangle$ in Eq. (22) via the unitary time-evolution operator $U_I(t)$

$$|\psi_I(t)\rangle = \sum_{M=-J}^{J} \sum_{n=0}^{\infty} \sum_{m_1=0}^{\infty} \sum_{m_2=0}^{\infty} C_M(0) C_{m_1 m_2}(0) U_{In}(t) |JM\rangle \otimes |m_1 m_2\rangle. \tag{40}$$

The different contributions to the interaction picture time evolution operator up to second-order are given by ($U_{I0} = 1$)

$$U_{I1}(t) = \sum_{j=1}^{2} \frac{G_j}{\sqrt{N}} (J_+ \otimes R_j^k \phi_j(t) - h.c.), \tag{41}$$

where the time-dependent first-order scalar function $\phi_j(t)$ is given by

$$\phi_j(t) = \frac{1 - e^{i\Delta_j t}}{\Delta_j}, \tag{42}$$

while the second-order contribution emerges as

$$U_{I2}(t) = \sum_{i=1}^{2}\sum_{j=1}^{2} \frac{G_i G_j}{N}[(J_+^2 \otimes R_i^k R_j^k \phi_{ij}^{++}(t) + J_+ J_- \otimes R_i^k R_j^{\dagger k} \phi_{ij}^{+-}(t)) + h.c.], \tag{43}$$

with the different signatures of the second-order time-dependent functions $\phi_{ij}(t)$ given by $(i, j = 1, 2; i \neq j)$

$$\phi_{ij}^{++}(t) = \frac{e^{i(\Delta_i+\Delta_j)t} - 1}{(\Delta_i + \Delta_j)\Delta_j} - \frac{e^{i\Delta_i t} - 1}{\Delta_i \Delta_j}, \tag{44}$$

$$\phi_{ij}^{+-}(t) = \frac{e^{i\Delta_i t} - 1}{\Delta_i \Delta_j} - \frac{e^{i(\Delta_i-\Delta_j)t} - 1}{(\Delta_i - \Delta_j)\Delta_j}, \tag{45}$$

$$\phi_{ij}^{-+}(t) = \phi_{ij}^{*+-}(t), \tag{46}$$

$$\phi_{ij}^{--}(t) = \phi_{ij}^{*++}(t), \tag{47}$$

$$\phi_{jj}^{+-}(t) = \frac{e^{i\Delta_j t} - 1 - it\Delta_j}{\Delta_j^2}. \tag{48}$$

Up to this point the developed formalism is completely general, allowing to investigate k photons transitions within the framework of time-dependent perturbation theory. The present study will be restricted to two-photon transitions, i.e., $k = 2$ in Eqs. (41) and (43). In real physical processes, the two-photon algebra acts on the harmonic-oscillator Fock space. Thus, matrix elements of the operators R_j^2, $R_i^2 R_j^2$, $R_i^2 R_j^{\dagger 2}$ and their hermitian conjugates implicit in Eqs. (41) and (43) are easily computed with respect to the standard number states $|n_i\rangle$ $(i = 1, 2)$ which form a basis for each subspace. Different contributions to the time-evolution operator matrix elements can be evaluated through

$$a_i^p |n_i\rangle = \sqrt{p! \binom{n_i}{p}} |n_i - p\rangle, \tag{49}$$

$$a_j^{\dagger q} |n_j\rangle = \frac{1}{\sqrt{(-q)! \binom{n_j}{-q}}} |n_j + q\rangle, \tag{50}$$

with $i, j = 1, 2$, $p \leq n_i$, and the matrix elements of the different radiation field operators acting on $|n_j\rangle$ are listed in Appendix A. With these ingredients and from the angular momentum coefficients

$$\lambda_{JM}^{\pm} = \sqrt{(J \mp M)(J \pm M + 1)}, \tag{51}$$

along with the definition emerging in the evaluation of matrix elements in the Fock space

$$Q_{n_j} = n_j (n_j - 1)^{1/2}, \tag{52}$$

the first- and second-order contributions to the time evolution operator matrix elements are obtained as

$$\begin{aligned} &\langle JM'| \otimes \langle m_1 m_2 | U_{I1}(t) | JM\rangle \otimes |n_1 n_2\rangle \\ &= \sum_{j\neq k}^{2} \frac{G_j}{\sqrt{N}} (\lambda_{JM}^{+} Q_{n_j} \phi_j(t) \delta_{M'M+1} \delta_{m_j n_j - 2} - \lambda_{JM}^{-} Q_{n_j+2} \phi_j^*(t) \delta_{M'M-1} \delta_{m_j n_j + 2}) \delta_{m_k n_k}, \end{aligned} \tag{53}$$

and

$$\begin{aligned}
&\langle JM'| \otimes \langle m_1 m_2|U_{I2}(t)|JM\rangle \otimes |n_1 n_2\rangle \\
&= \sum_{j\neq k}^{2}\Bigg[\frac{G_j^2}{N}(\lambda_{JM}^{+}\lambda_{JM+1}^{+}Q_{n_j}Q_{n_j-2}\phi_{jj}^{++}(t)\delta_{M'M+2}\delta_{m_j n_j-4} \\
&\quad + (\lambda_{JM}^{-}\lambda_{JM-1}^{+}Q_{n_j+2}^{2}\phi_{jj}^{*+-}(t) + \lambda_{JM}^{+}\lambda_{JM+1}^{-}Q_{n_j}^{2}\phi_{jj}^{-+}(t))\delta_{M'M}\delta_{m_j n_j} \\
&\quad + \lambda_{JM}^{-}\lambda_{JM-1}^{-}Q_{n_j+2}Q_{n_j+4}\phi_{jj}^{--}(t)\delta_{M'M-2}\delta_{m_j n_j+4})\delta_{m_k n_k} \\
&\quad + \frac{G_j G_k}{N}(\lambda_{JM}^{+}\lambda_{JM+1}^{+}Q_{n_j}Q_{n_k}\phi_{jk}^{++}(t)\delta_{M'M+2}\delta_{m_j n_j-2}\delta_{m_k n_k-2} \\
&\quad + \lambda_{JM}^{-}\lambda_{JM-1}^{+}Q_{n_j+2}Q_{n_k}\phi_{jk}^{+-}(t)\delta_{M'M}\delta_{m_j n_j-2}\delta_{m_k n_k+2} \\
&\quad + \lambda_{JM}^{+}\lambda_{JM+1}^{-}Q_{n_j}Q_{n_k+2}\phi_{jk}^{-+}(t)\delta_{M'M}\delta_{m_j n_j+2}\delta_{m_k n_k-2} \\
&\quad + \lambda_{JM}^{-}\lambda_{JM-1}^{-}Q_{n_j+2}Q_{n_k+2}\phi_{jk}^{--}(t)\delta_{M'M-2}\delta_{m_j n_j+2}\delta_{m_k n_k+2})\Bigg].
\end{aligned} \tag{54}$$

Note that the different contributions of the time evolution operator act on the ensemble of the totality of angular momentum states $|JM\rangle$ and not merely on the ground state $M=-J$, the fully excited state $M=J$, or the half-excited Dicke state $M=0$. The collective effects for different initial atomic states were studied in detail some time ago [8]. It was claimed that if the atoms are prepared initially in the ground state ($M=-J$) or in the fully excited state ($M=J$), then the system behaves rather similarly to the single-atom case. But, the results are different when the atoms are prepared initially in the half-excited Dicke state ($M=0$). This state is well known as the superradiant atomic state in the context of collective spontaneous emission in open space. In the present study, the global initial state is given by the tensor product of the simultaneous superposition of the totality of Dicke atomic states $|JM\rangle$ and the field modes, given in terms of Glauber coherent states as Eq. (22) shows.

The time-dependent density operator emerges as the perturbative solution of the Heisenberg equation of motion via

$$\begin{aligned}
\rho(t) &= e^{-i\hat{\mathcal{V}}(t)}\rho(0) \\
&= 1 - i[\mathcal{V}(t),\rho(0)] + \frac{(-i)^2}{2!}[\mathcal{V}(t),[\mathcal{V}(t),\rho(0)]] + \cdots,
\end{aligned} \tag{55}$$

where $\hat{\mathcal{V}}(t)$ is a superoperator defined by $\hat{\mathcal{V}}(t)\rho(0) = [\mathcal{V}(t),\rho(0)]$. Truncated to second-order, the matrix elements of this density operator are given by

$$\rho_{MM'}^{n_1 m_1 n_2 m_2}(t) = C_{M'}^{m_1 m_2}(t)C_{M}^{n_1 n_2}(t), \tag{56}$$

with the coefficients

$$\begin{aligned}
C_{M'}^{m_1 m_2}(t) &= C_{M'}(0)[\rho_{m_1 m_1}^{f}(0)\rho_{m_2 m_2}^{f}(0)]^{1/2} \\
&\quad + \sum_{j\neq k}^{2}\Bigg[\frac{G_j}{\sqrt{N}}(\lambda_{JM'-1}^{+}Q_{m_j+2}\phi_j(t)C_{M'-1}(0)[\rho_{m_j+2 m_j+2}^{f}(0)\rho_{m_k m_k}^{f}(0)]^{1/2} \\
&\quad - \lambda_{JM'+1}^{-}Q_{m_j}\phi_j^{*}(t)C_{M'+1}(0)[\rho_{m_j-2 m_j-2}^{f}(0)\rho_{m_k m_k}^{f}(0)]^{1/2}) \\
&\quad + \frac{G_j^2}{N}(\lambda_{JM'-2}^{+}\lambda_{JM'-1}^{+}Q_{m_j+4}Q_{m_j+2}\phi_{jj}^{++}(t)C_{M'-2}(0) \\
&\quad \times [\rho_{m_j+4 m_j+4}^{f}(0)\rho_{m_k m_k}^{f}(0)]^{1/2} + (\lambda_{JM'}^{-}\lambda_{JM'-1}^{+}Q_{m_j+2}^{2}\phi_{jj}^{+-}(t) \\
&\quad + \lambda_{JM'}^{+}\lambda_{JM'+1}^{-}Q_{m_j}^{2}\phi_{jj}^{-+}(t))C_{M'}(0)[\rho_{m_j m_j}^{f}(0)\rho_{m_k m_k}^{f}(0)]^{1/2} \\
&\quad + \lambda_{JM'+2}^{-}\lambda_{JM'+1}^{-}Q_{m_j-2}Q_{m_j}\phi_{jj}^{--}(t)C_{M'+2}(0)[\rho_{m_j-4 m_j-4}^{f}(0)\rho_{m_k m_k}^{f}(0)]^{1/2})
\end{aligned}$$

$$+\frac{G_jG_k}{N}(\lambda^{+}_{JM'-2}\lambda^{+}_{JM'-1}Q_{m_j+2}Q_{m_k-2}\phi^{++}_{jk}(t)C_{M'-2}(0)[\rho^{f}_{m_j+2m_j+2}(0)\rho^{f}_{m_k+2m_k+2}(0)]^{1/2}$$
$$+\lambda^{-}_{JM'}\lambda^{+}_{JM'-1}Q_{m_j+4}Q_{m_k-2}\phi^{+-}_{jk}(t)C_{M'}(0)[\rho^{f}_{m_j+2m_j+2}(0)\rho^{f}_{m_k-2m_k-2}(0)]^{1/2}$$
$$+\lambda^{+}_{JM'}\lambda^{-}_{JM'+1}Q_{m_j-2}Q_{m_k+4}\phi^{-+}_{jk}(t)C_{M'}(0)[\rho^{f}_{m_j-2m_j-2}(0)\rho^{f}_{m_k+2m_k+2}(0)]^{1/2}$$
$$+\lambda^{-}_{JM'+2}\lambda^{-}_{JM'+1}Q_{m_j}Q_{m_k}\phi^{--}_{jk}(t)C_{M'+2}(0)\ [\rho^{f}_{m_j-2m_j-2}(0)\rho^{f}_{m_k-2m_k-2}(0)]^{1/2})\Big]. \quad (57)$$

The rather complex structure of the density operator matrix elements shows that the model becomes strongly entangled at times $t > 0$, which is reflected in the behavior of the time evolution of the linear entropy and of other nonclassical effects, as discussed in the next section.

3. Results and discussion

In the computations to be described below, the density operator matrix elements of the field at $t = 0$ are given in terms of the Poisson distribution of Eq. (20)

$$\rho^{f}_{n_jn_j}(0) = \frac{\overline{n}_j^{n_j}e^{-\overline{n}_j}}{n_j!}, \quad (58)$$

where $\overline{n}_j$ ($\equiv|z_j|^2$) is the initial mean photon number. The model parameters will be characterized in terms of the strength of the coupling as measured by the dimensionless ratio $\kappa_i = G_i/(\omega - 2\nu_i)$.

The photon number distribution is a stationary property. Thus, computation of this quantity can be realized at any arbitrary time. In Fig. 1, we plot the photon number distribution for the initial state (i.e. $t = 0$) as given by

$$p(n_1) = \sum_{n_2=0}^{\infty} Tr^{S}\rho(0) \equiv \sum_{n_2=0}^{\infty}\sum_{M=-j}^{J}\rho^{n_1n_1n_2n_2}_{MM}(0), \quad (59)$$

in terms of the photon number for the first mode n_1 and for three different values of the initial mean photon number $\overline{n}_1$. In Eq. (59), the superscript S stands for the bosonic system S and Tr^S is the partial trace over the degrees of freedom of the ensemble of N two-level atoms. Since the photon distribution is not a dynamical quantity, the calculations can be performed in the strong coupling limit, without altering the spirit of the perturbative treatment of the model. In the present case, we take $\kappa_1 = 47$ and $\kappa_2 = 12$. The computations were performed by averaging over n_2, the photon quantum number for the second mode. It is observed that the Poisson distributions peak at the integer value closest to $\overline{n}_1$. As expected, the amplitudes decrease with the increase of $\overline{n}_1$ and a consequent increase in the half-width of the distribution, thus preserving the normalization of the state.

We next examine the spin and field squeezing. The uncertainty principle limits the precise knowledge of all physical quantities in a quantum system. One tool often used to *overcome* the restrictions imposed by the uncertainty principle in practical quantum applications is the squeezed states. These nonclassical states are characterized when the variance for a given quadrature operator, calculated using them, is amplified while the variance in the other quadrature operator is deamplified, keeping their product bounded by the uncertainty principle. The Bloch states form minimum uncertainty packets. The uncertainty relation can be defined in terms of the set of rotated operators

$$\begin{pmatrix} J_\chi \\ J_\xi \\ J_\zeta \end{pmatrix} = R_{\theta,\phi}\begin{pmatrix} J_x \\ J_y \\ J_z \end{pmatrix}R^{-1}_{\theta,\phi}. \quad (60)$$

These three observables obey a commutation relation of the type $[A, B] = iC$ with $A = J_\chi$, $B = J_\xi$, $C = J_\zeta$, whence they have the uncertainty property

$$\Delta J_\chi\,\Delta J_\xi \geq \frac{1}{2}|\langle J_\zeta\rangle|, \quad (61)$$

for any states. It is easy to show that the equality sign holds for the Bloch state $|\theta, \phi\rangle$, which is therefore a minimum-uncertainty state.

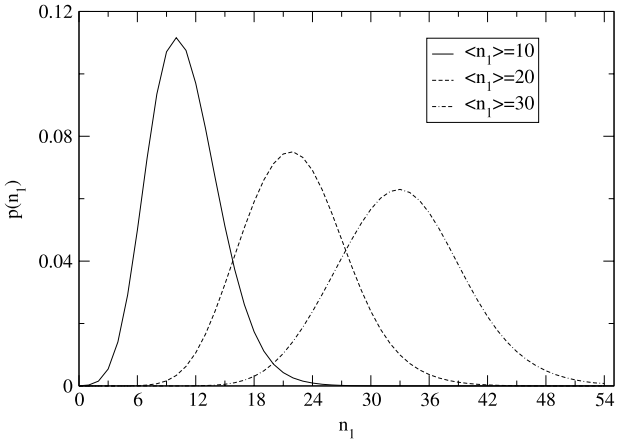

Fig. 1. Photon distribution of the Dicke model for three different values of the mean photon number $\langle n_1\rangle \equiv \bar{n}_1$ in the initial state. The initial mean photon number for the second mode is $\bar{n}_2 = 12$. The system is initially prepared in coherent superposition states of angular momentum $|JM\rangle$ with $J = 20$ interacting dispersively with the coherent field given by a Poisson distribution. $\omega = 83\ \mathrm{cm}^{-1}$; $\nu_1 = 37\ \mathrm{cm}^{-1}$; $\nu_2 = 74\ \mathrm{cm}^{-1}$; $G_1 = 467\ \mathrm{cm}^{-1}$; $G_2 = 800\ \mathrm{cm}^{-1}$; $\theta = \pi/4$; $\phi = \pi/3$.

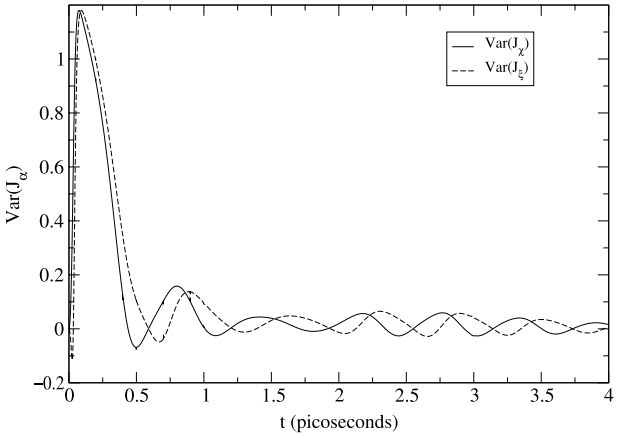

Fig. 2. Time evolution of the variance squeezing factor $Var(J)$ based on the Heisenberg uncertainty relation. The system is initially prepared in coherent superposition states of angular momenta $|JM\rangle$ with $J = 3$ interacting dispersively with the coherent field given by a Poisson distribution. $\omega = 5000\ \mathrm{cm}^{-1}$; $\nu_1 = 1367\ \mathrm{cm}^{-1}$; $\nu_2 = 743\ \mathrm{cm}^{-1}$; $G_1 = 4.67\ \mathrm{cm}^{-1}$; $G_2 = 8\ \mathrm{cm}^{-1}$; $\theta = \pi$; $\phi = \pi/4$. The initial mean photon numbers are $\bar{n}_1 = 20$ and $\bar{n}_2 = 10$.

Fluctuations in the component J_α ($\alpha = \chi, \xi$ or x, y) of the atomic dipole are said to be squeezed if J_α satisfies the condition

$$Var(J_\alpha) = \Delta J_\alpha - \left(\frac{|\langle J_\zeta\rangle|}{2}\right)^{1/2} < 0, \tag{62}$$

where $\Delta J_\alpha = [\langle J_\alpha^2\rangle - \langle J_\alpha\rangle^2]^{1/2}$. General expressions valid to all orders that are necessary to compute second-order statistical moments for the different angular momentum components are derived in Appendix B. Fig. 2 displays the time evolution of the fluctuations in the components J_α ($\alpha = \chi, \xi$) in the limit of a rather weak coupling for both modes $\kappa_1 = 0.20 \times 10^{-2}, \kappa_2 = 0.23 \times 10^{-2}$. The atomic system is initially in superposition states $|JM\rangle$ and the field is in a coherent state. It can be observed that the second-order variance $Var(J_\alpha)$ predicts no squeezing in the J_χ component at times smaller than 0.5 ps, and after that it oscillates with amplitudes that get smaller with the passage of time. The squeezing

only appears during short periods of time, keeping the magnitude of the fluctuations above and below of zero with a nearly constant period above 2 ps. The J_ξ component, on the other hand, predicts a small amount of continuous squeezing only at transient times less than 0.1 ps. In the neighborhood of zero and at times longer than 2 ps, both components are alternatively squeezed and unsqueezed, thus preserving the uncertainty relation given by Eq. (61). These CSS have an isotropic quasiprobability distribution in a spherical phase space [41] and in these systems squeezing occurs on this phase sphere. Unlike boson squeezing, this quasiprobability distribution cannot be homogeneously or globally squeezed in one direction over the whole phase space. If an angular momentum or spin component is shrunk around a certain point on the sphere, it must be stretched around another point, what then imposes a fundamental restriction on the reduction in quantum noise.

We now focus on the important quantum phenomenon of field squeezing. The initially coherent cavity field can be squeezed when it interacts with a single atom [36,42], and squeezing in the revival-time regime can be very strong for large intensities of the field [43,44]. Fig. 3 shows the normal squeezing factor of the field in the quadrature modes

$$X_1^{(i)}(t) = \frac{1}{2}(a_i e^{i2\nu_i t} + a_i^\dagger e^{-i2\nu_i t}), \tag{63}$$

$$X_2^{(i)}(t) = -\frac{i}{2}(a_i e^{i2\nu_i t} - a_i^\dagger e^{-i2\nu_i t}). \tag{64}$$

These operators satisfy the canonical commutation relations

$$[X_1^{(i)}(t), X_2^{(j)}(t)] = \frac{i}{2}\delta_{ij}, \tag{65}$$

which implies the uncertainty relations

$$\langle(\Delta X_1^{(i)})^2\rangle\langle(\Delta X_2^{(i)})^2\rangle \geq \frac{1}{16}. \tag{66}$$

Squeezing is said to exist whenever the uncertainty of one of the quadratures is below the vacuum level (standard quantum limit), i.e., $\langle(\Delta X_j^{(i)})^2\rangle < \frac{1}{4}$. In order to characterize the influence of intrinsic decoherence on the squeezing, it was found convenient to characterize the squeezing through the use of the parameter ($Q_{ij} \equiv Q_{ij}(t)$)

$$Q_{ij} = 1 - 4\langle(\Delta X_j^{(i)})^2\rangle, \tag{67}$$

where $0 < Q_{ij} \leq 1$ for squeezing. The computations were conducted in the coupling limits $\kappa_1 = 0.25 \times 10^{-2}$ and $\kappa_2 = 1.2$. It was claimed [45] that in the Dicke model collective atomic effects can improve squeezing obtained for short interaction times, compared to the single-atom case. It is found that the present model only gives a certain amount of squeezing (less than 20%) for times longer than 0.1 ps approximately, which is due to the two-mode two-photon process we are considering. In fact, squeezing depends on two-photon transitions, when a pair of photons is simultaneously absorbed or emitted by the atomic system. The oscillations of $Q_{21}(t)$ decay with time but their regular pattern is conserved on the long-time scale. This decay is correlated with the regularity in the behavior of the atomic inversion, caused by very large overlaps of neighboring revivals. Fig. 4 shows the atomic inversion as given by the third part of Eq. (B.22). A rapid decay of the atomic inversion with the passage of time is observed. In the many-atom case there exist anharmonic collective corrections (not taken into account in the present study) which modify the shape of the atomic inversion related to the photon-distribution mechanism [46].

It is well known that the revivals of the atomic inversion as well as the oscillations in the photon number distribution in Jaynes–Cummings models arise as a consequence of quantum interference in phase space. These nonclassical effects have their origin in quantum coherences established during the interaction between the atom and the cavity field [47]. From the structure of the time-dependent density operator matrix elements, it is evident that its high degree of entanglement contributes to the destruction of quantum coherences. This leads to the appearance of "decay" factors in the term $\langle J_z\rangle$ which is responsible for the destruction of revivals of the atomic inversion. In other words, with a

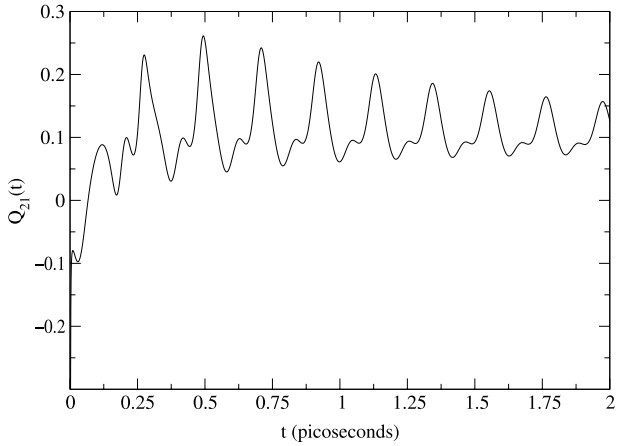

Fig. 3. Time evolution of the normal second-order squeezing factor $Q_{21}(t)$. The system is initially prepared in coherent superposition states of angular momenta $|JM\rangle$ with $J = 5$ interacting dispersively with the coherent field given by a Poisson distribution. $\omega = 833\ \mathrm{cm}^{-1}$; $\nu_1 = 1367\ \mathrm{cm}^{-1}$; $\nu_2 = 743\ \mathrm{cm}^{-1}$; $G_1 = 4.67\ \mathrm{cm}^{-1}$; $G_2 = 800\ \mathrm{cm}^{-1}$; $\theta = \pi/4$; $\phi = \pi/3$. The initial mean photon numbers are $\overline{n}_1 = 20$ and $\overline{n}_2 = 10$.

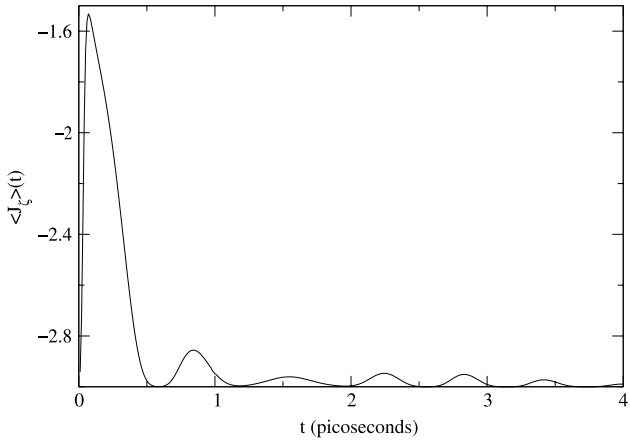

Fig. 4. Time evolution of the atomic inversion $\langle J_\zeta \rangle(t)$. The system is initially prepared in coherent superposition states of angular momenta $|JM\rangle$ with $J = 3$ interacting dispersively with the coherent field given by a Poisson distribution. The value of the different parameters is the same as those given in Fig. 2.

rapid suppression of quantum coherences, we can observe rapid deterioration of revivals of the atomic inversion. Fig. 4 illustrates the decay of quantum coherences due to the very specific time evolution described by the density matrix elements involved in $\langle J_z \rangle$, i.e., due to the intrinsic decoherence. Of course, the system remains conservative, so there is no dissipation of energy and the inversion "relaxes" to the asymptotic $|J|$ value.

We now study the dynamics of the field statistics of this generalized Dicke model, with particular attention to the production of states of the field exhibiting nonclassical properties. Nonclassical effects were previously detected in the investigation of the dynamics of the Raman coupled model interacting with two quantized cavity fields [48]. To characterize the statistical properties of the light beams, we introduce the function

$$\gamma_{ij}^{(2)} = \frac{\langle a_i^\dagger(t) a_j^\dagger(t) a_j(t) a_i(t) \rangle}{\langle a_i^\dagger(t) a_i(t) \rangle \langle a_j^\dagger(t) a_j(t) \rangle}, \quad i, j = 1, 2. \tag{68}$$

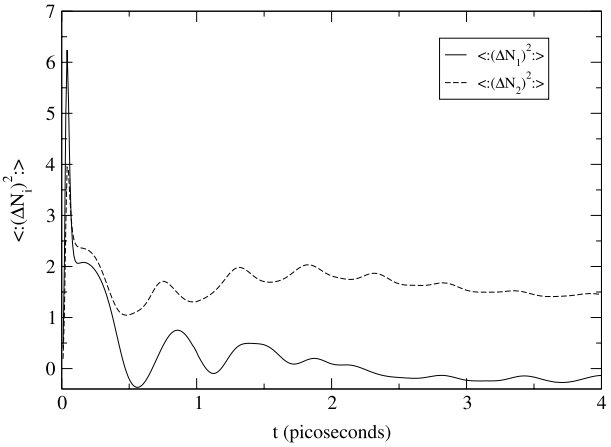

Fig. 5. Time evolution of the normally ordered photon number variance. The system is initially prepared in coherent superposition states of angular momenta $|JM\rangle$ with $J = 3$ interacting dispersively with the coherent field given by a Poisson distribution. The value of the different parameters is the same as those given in Fig. 2.

Here $\gamma_{ii}^{(2)}$ defines the degrees of second-order coherence in the modes and $\gamma_{12}^{(2)}$ describes the degree of intermode correlation.

We first consider the second-order coherence of the modes. The function $\gamma_{ii}^{(2)}$ can be written in terms of the normally ordered photon number variance $\langle : (\Delta N_i)^2 : \rangle$ as

$$\gamma_{ii}^{(2)} = 1 + \frac{\langle : (\Delta N_i)^2 : \rangle}{\langle N_i \rangle^2}, \tag{69}$$

where $N_i = a_i^\dagger a_i$ and

$$\langle : (\Delta N_i)^2 : \rangle = \langle a_i^\dagger(t) a_i^\dagger(t) a_i(t) a_i(t) \rangle - \langle N_i \rangle^2. \tag{70}$$

The light is nonclassical, exhibiting the sub-Poisson statistics whenever $\gamma_{ii}^{(2)} < 1$ or equivalently whenever $\langle : (\Delta N_i)^2 : \rangle < 0$. Time evolution of the normally ordered variances of the photon number operators is presented in Fig. 5. In this figure the coupling parameters, the average quantum numbers of the field, the total angular momentum, as well as the angles θ, ϕ are the same as those used in Fig. 2. It appears, from Fig. 5, that for the particular set of parameters used, sub-Poisson statistics will always be present in the first mode for times longer than 2 ps. In the neighborhood of $t = 0.5$ ps it is observed a rather pronounced sub-Poissonian statistics. We notice that the second mode shows no antibunching over the whole time scale considered. In other words, no antibunching is observed in this mode but dominates slightly the first mode. We observe that the antibunching in the first mode occurs in regions where the atomic inversion $\langle J_\zeta \rangle$ evolves to values very close to $|J_\zeta| = J$.

Also of interest is the degree of interbeam second-order coherence. We actually calculate the cross-correlation function (or the covariance of the product of the photon number operators) between the two modes as defined by

$$C(t) = \langle a_1^\dagger(t) a_2^\dagger(t) a_2(t) a_1(t) \rangle - \prod_{i=1}^{2} \langle a_i^\dagger(t) a_i(t) \rangle, \tag{71}$$

which is proportional to the excess coincidence counting rate for a Hanbury–Brown–Twiss-type experiment with two beams. For $C(t) = 0$ the beams are uncorrelated ($\gamma_{12}^{(2)} = 0$), for $C(t) > 0$ they are correlated ($\gamma_{12}^{(2)} > 0$), and for $C(t) < 0$ they are anticorrelated ($\gamma_{12}^{(2)} < 0$). Because of the nature of the interaction in the present model, where one photon is associated with each single mode, we expect the two modes to be predominantly anticorrelated. This is evident in Fig. 6, where we plot the time evolution of $C(t)$ vs. t.

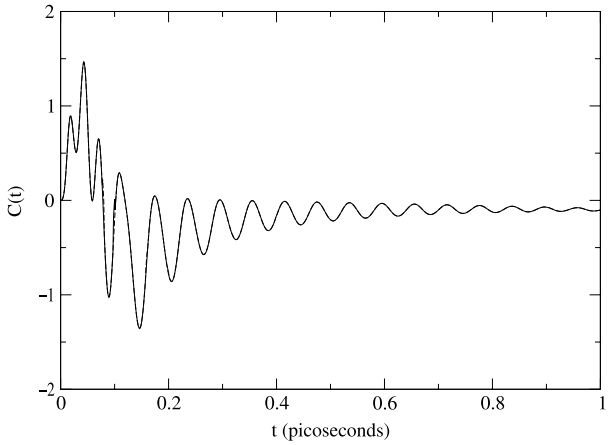

Fig. 6. Time evolution of the cross-correlation function. The system is initially prepared in coherent superposition states of angular momenta $|JM\rangle$ with $J = 3/2$ (solid line) and $J = 5/2$ (dashed line) interacting dispersively with the coherent field given by a Poisson distribution. The value of the different parameters is the same as those given in Fig. 2.

Decoherence, leading to the quantum superpositions turning into a statistical mixture is an important factor that helps to understand the behavior of the interaction in the long time regime. The characteristic time of decoherence is less than the decay time by a factor characterizing the "separation" between different parts of the quantum superposition. These features can be clearly observed in Figs. 4–6. First, there is a fast decay of nondiagonal elements of the field density matrix in the coherent states basis in the course of free evolution of the quantized field. Second, there is a rapid loss of mutual coherence between semiclassical states in the model. Because of the interference between two adjacent semiclassical states that leads to the appearance of the collapse-revival structure, the decoherence observed in Figs. 4–6 is reflected in a strong suppression of revival amplitudes. In other words, any intrinsic decoherence will not only reduce the superposition to a statistical mixture, but also eliminate the revival consequent upon the survival of the superposition. This intrinsic decoherence also modifies the time evolution of the atomic inversion, as Fig. 4 shows.

We now consider the Cauchy–Schwartz inequality

$$(\gamma_{12}^{(2)})^2 \leq \gamma_{11}^{(2)}\gamma_{22}^{(2)}, \tag{72}$$

which is violated by nonclassical states, indicating a nonclassical correlation between the beams. We actually calculate the quantity

$$V(t) = \langle a_1^\dagger(t)a_2^\dagger(t)a_2(t)a_1(t)\rangle^2 - \prod_{i=1}^{2}\langle a_i^\dagger(t)a_i^\dagger(t)a_i(t)a_i(t)\rangle. \tag{73}$$

Whenever $V(t)$ is positive, the inequality in Eq. (72) is violated. In Fig. 7, it can be observed that, effectively, this inequality is slightly violated in the long time regime and this violation is more pronounced for $J = 5/2$ than for $J = 3/2$ above $t \sim 0.5$ ps. In the very short time regime it appears not to be violated at all.

We now turn to investigate the dynamics of entanglement. To study dynamics of entanglement, one must choose an entanglement measure. In the present case, the entanglement can be described by the linear entropy or the von Neumann entropy. A similar behavior of the two measures is found. Thus we only present the results of the linear entropy. In fact, the evaluation of the entanglement dynamics in terms of the linear entropy results to be much less demanding from the computational point of view, not requiring the diagonalization of the density matrix. This aspect appears to be relevant since the complexity of many systems of physical interest practically prevents the diagonalization of the corresponding density matrix [49].

The linear entropy is a measure of mixedness in quantum states. It is a scalar defined as [50]

$$S_L(t) = 1 - Tr^S\rho^S(t)^2, \tag{74}$$

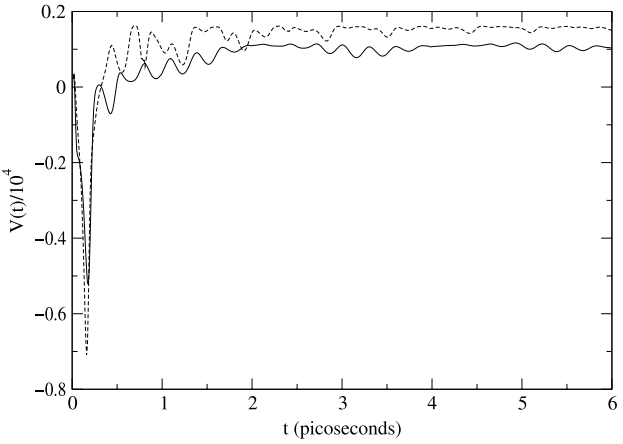

Fig. 7. Behavior of the Cauchy–Schwartz inequality $V(T)$ vs. t. The system is initially prepared in coherent superposition states of angular momenta $|JM\rangle$ with $J = 3/2$ (solid line) and $J = 5/2$ (dashed line) interacting dispersively with the coherent field given by a Poisson distribution. The value of the different parameters is the same as those given in Fig. 3, except $G_2 = 8\ \mathrm{cm}^{-1}$.

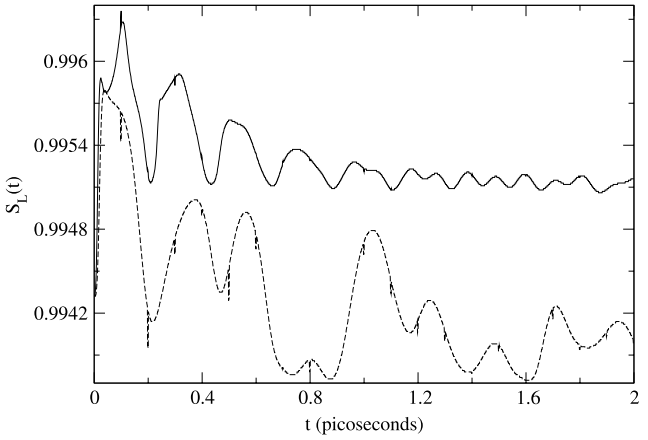

Fig. 8. Time evolution of the linear entropy. The system is initially prepared in coherent superposition states of angular momenta $|JM\rangle$ with $J = 5$ (solid line) and $J = 5/2$ (dashed line) interacting dispersively with the coherent field given by a Poisson distribution. The value of the different parameters is the same as those given in Fig. 3, except $G_2 = 8\ \mathrm{cm}^{-1}$, $\theta = \pi/2$, $\phi = \pi$.

where $\rho^S(t)$ is the reduced density matrix $\rho^S(t) = Tr^f |\psi_I(t)\rangle\langle\psi_I(t)|$, with $|\psi_I(t)\rangle$ the quantum state of the full system [Eq. (40)], which evolves in time under the action of the evolution operator $U_I(t)$ of Eq. (38). We note that the expression of $S_L(t)$ is representation-independent since the trace is invariant under unitary transformations of the model. In the language of entanglement $S_L(t)$ ranges from 0 (i.e., $Tr\,\rho(t)^2 = 1$) for disentangled and/or pure states to 1 (i.e., $Tr\,\rho(t)^2 = 0$) for maximally entangled bipartite. Thus, $Tr\,\rho(t)^2$ can be taken as the Bloch sphere radius introduced in Section 2.

The entanglement entropy was recently studied in the context of the Bose–Einstein condensate [32]. Our aim here is to investigate the time evolution of the atomic and field initially coherent states along with the occurrence of entanglement between both systems. Thus, we let the model evolve by means of the evolution operator in Eq. (40) and explore the entanglement dynamics by tracing out the field and atomic density operators over the corresponding degrees of freedom.

Fig. 8 displays the numerical results of the linear entropy for two different values of the total angular momentum J. The computations were conducted in the weak coupling limit for both modes, i.e., $\kappa_1 = 0.25 \times 10^{-3}$ and $\kappa_2 = 0.12 \times 10^{-1}$.

It can be observed that entanglement has a rapid rise after a very short initial time for both $J = 5$ and $J = 5/2$. When $J = 5$, i.e., $N = 10$, the entropy saturates to a relatively stable value with continuous oscillations of small amplitudes. With a decrease in the number of atoms to $N = 5$, which corresponds to a total angular momentum $J = 5/2$, strong oscillations of entanglement with the magnitude of the entropy keeping below the $J = 5$ case for the whole time scale considered are observed. The maximal entanglement $S_{L\ max}$ here can be considered as entangling powers of unitary operations, describing the capability of entropy production. The maximal entanglement increases with J, i.e., with the number of atoms, passing from 0.9955 for $J = 5/2$ to 0.9967 for $J = 5$. In both cases, it is noted that the linear entropy monotonically approaches a plateau as it should be for an irreversible process. In fact, at the end of the standard relaxation process the linear entropy reaches a sort of thermodynamic equilibrium and all the revivals are suppressed. It is clear that the collapse is now irreversible due to the subsequent incoherence of possible chaotic trajectories.

It is well known that statistical mixtures correspond to points *inside* the Bloch sphere on the z-axis. Statistical mixtures therefore have $r < 1$, in contrast to superposition states, which are always on the surface of the sphere with $r = 1$. The pattern in Fig. 8 is reminiscent of damping processes which destroy coherence and reduce superposition states to statistical mixtures. Since statistical mixtures have $r < 1$, Fig. 8 shows that the Dicke model does not preserve the modulus of the Bloch vector. This entanglement is a sort of accessible entanglement, i.e., the maximum value of the entanglement that could be extracted from the system and placed in quantum registers, from which it could be used to perform quantum information processing.

4. Conclusions

In this paper, a previously univestigated novel procedure, based on the perturbative solution of the time-dependent (interaction picture representation) Schrödinger equation was introduced to study the possible existence of nonclassical effects emerging from the dispersive interaction of N two-level atoms with a bimodal cavity field. One of the novel features of the model is the incorporation of intensity dependent photon operators in the interactive part of the Dicke Hamiltonian. The resulting highly nonlinear generalized Dicke model involves two-photon transitions in a scenario where the RWA is assumed. The homogeneity of the model allowed us to represent the Dicke Hamiltonian entirely in terms of the total angular momentum J. The computations were conducted via second-order Dyson perturbative expansion of the time evolution operator matrix elements for the totality of angular momentum states of the atomic system. It was assumed that, initially, the atomic system and the field are in a disentangled state, with the boson field in the Glauber coherent state and the atomic system in an ensemble of Dicke states $JM > (-J \leq M \leq J)$. At $t > 0$ the resulting time-dependent density operator matrix becomes strongly entangled. This is reflected in a number of nonclassical properties such as spin and field squeezing, photon antibunching as well as violation of the Cauchy–Schwartz inequality in the long time regime. The disentanglement, resulting from the irreversible coupling of the atomic system with the degrees of freedom of the cavity field, produces the phenomenon of decoherence that leads to the quantum superpositions turning into a statistical mixture. This phenomenon is reflected in the time evolution of the linear entropy, where it is clearly observed that the present model does not preserve the modulus of the Bloch vector. Thus, the results obtained lead to the conclusion that the linear entropy can be an efficient and still valid entanglement measure for Dicke models, as for other physical phenomena of interest in quantum-information processing.

Finally, it should be stressed that it is of great interest to explore approximate solutions of more complex Hamiltonians that contain the counter-rotating terms [51] for a wide range of the system parameters, and compare them with the RWA results. Work along these lines is underway and will be reported elsewhere.

Acknowledgments

The author is extremely grateful to Lorena Rebon, Department of Physics, University of La Plata, Argentina, for stimulating discussions about this work. This project is supported by research grants in aid from the University of Buenos Aires (Project No. X-017/08), and the Consejo Nacional de

Investigaciones Científicas y Técnicas (CONICET, PIP No. 11220090100061/10). The author is grateful to the Department of Physics, Facultad de Ciencias Exactas y Naturales, University of Buenos Aires, for facilities provided during the course of this work.

Appendix A. Radiation field operators matrix elements in the fock space

The radiation field operators' matrix elements in the Fock space are computed from Eqs. (49)–(50). They are given in terms of the parameters Q_{n_j} of Eq. (52) as

$$\langle m_j m_k|R_j^2|n_j n_k\rangle = Q_{n_j}\delta_{m_j n_j-2}\delta_{m_k n_k},$$
$$\langle m_j m_k|R_j^{\dagger 2}|n_j n_k\rangle = Q_{n_j+2}\delta_{m_j n_j+2}\delta_{m_k n_k},$$
$$\langle m_j m_k|R_j^2 R_k^2|n_j n_k\rangle = Q_{n_j}Q_{n_k}\delta_{m_j n_j-2}\delta_{m_k n_k-2},$$
$$\langle m_j m_k|R_j^2 R_k^{\dagger 2}|n_j n_k\rangle = Q_{n_j}Q_{n_k+2}\delta_{m_j n_j-2}\delta_{m_k n_k+2},$$
$$\langle m_j m_k|R_j^{\dagger 2} R_k^2|n_j n_k\rangle = Q_{n_j+2}Q_{n_k}\delta_{m_j n_j+2}\delta_{m_k n_k-2},$$
$$\langle m_j m_k|R_j^{\dagger 2} R_k^{\dagger 2}|n_j n_k\rangle = Q_{n_j+2}Q_{n_k+2}\delta_{m_j n_j+2}\delta_{m_k n_k+2},$$
$$\langle m_j m_k|R_j^4|n_j n_k\rangle = Q_{n_j}Q_{n_j-2}\delta_{m_j n_j-4}\delta_{m_k n_k},$$
$$\langle m_j m_k|R_j^2 R_j^{\dagger 2}|n_j n_k\rangle = Q_{n_j+2}^2\delta_{m_j n_j}\delta_{m_k n_k},$$
$$\langle m_j m_k|R_j^{\dagger 2} R_j^2|n_j n_k\rangle = Q_{n_j}^2\delta_{m_j n_j}\delta_{m_k n_k},$$
$$\langle m_j m_k|R_j^{\dagger 4}|n_j n_k\rangle = Q_{n_j+2}Q_{n_j+4}\delta_{m_j n_j+4}\delta_{m_k n_k}.$$

To derive explicit expressions for the second-order coherence given in Eq. (68) we proceed as follows. The average photon numbers $\overline{n}_i(t)$ $(i = 1, 2)$ are obtained as

$$\overline{n}_i(t) = \sum_{n_1=0}^{\infty}\sum_{n_2=0}^{\infty}\sum_{M=-J}^{J} n_i \rho_{MM}^{n_1 n_1 n_2 n_2}(t), \tag{A.1}$$

and where $\overline{n}_i(0) \equiv \overline{n}_i$. The expectation values $\langle N_i\rangle \equiv \overline{n}_i(t)$ appearing in Eq. (69) are just those given by Eq. (A.1) while the first term on the right of Eq. (70) is given by

$$\langle a_i^\dagger(t)a_i^\dagger(t)a_i(t)a_i(t)\rangle = \sum_{n_1=0}^{\infty}\sum_{n_2=0}^{\infty}\sum_{M=-J}^{J} n_i(n_i-1)\rho_{MM}^{n_1 n_1 n_2 n_2}(t). \tag{A.2}$$

Finally, the first term on the right in Eq. (71) is straightforwardly computed as

$$\langle a_1^\dagger(t)a_2^\dagger(t)a_2(t)a_1(t)\rangle = \sum_{n_1=0}^{\infty}\sum_{n_2=0}^{\infty}\sum_{M=-J}^{J} n_1 n_2 \rho_{MM}^{n_1 n_1 n_2 n_2}(t). \tag{A.3}$$

Appendix B. Important relations concerning rotated operators

Investigation of the variances containing second-order statistical moments in the angular momentum components (J_x, J_y, J_z) and their rotated counterparts (J_χ, J_ξ, J_ζ) requires the computation of a number of matrix elements of these operators in the basis given by the interaction picture Dicke wavefunction given in Eq. (40).

It is first observed, with the help of Eq. (51), that matrix elements of J_+^2, J_+J_-, and their hermitian conjugates, are easily evaluated as

$$\langle JM'|J_+^2|JM\rangle = \lambda_{JM}^+\lambda_{JM+1}^+\delta_{M'M+2}, \tag{B.1}$$
$$\langle JM'|J_-^2|JM\rangle = \lambda_{JM}^-\lambda_{JM-1}^-\delta_{M'M-2}, \tag{B.2}$$

$$\langle JM'|J_+J_-|JM\rangle = \lambda^-_{JM}\lambda^+_{JM-1}\delta_{M'M}, \tag{B.3}$$

$$\langle JM'|J_-J_+|JM\rangle = \lambda^+_{JM}\lambda^-_{JM+1}\delta_{M'M}. \tag{B.4}$$

From the definitions $J_x = 1/2(J_+ + J_-)$, $J_y = 1/2i(J_+ - J_-)$ along with the relation $\lambda^+_{JM} = \lambda^-_{JM+1}$ and after some algebra one gets

$$\langle J_x\rangle = Re\sum_{n_1=0}^{\infty}\sum_{n_2=0}^{\infty}\sum_{M=-J}^{J}\rho^{n_1n_1n_2n_2}_{MM+1}(t)\lambda^+_{JM}, \tag{B.5}$$

$$\langle J_y\rangle = Im\sum_{n_1=0}^{\infty}\sum_{n_2=0}^{\infty}\sum_{M=-J}^{J}\rho^{n_1n_1n_2n_2}_{MM+1}(t)\lambda^+_{JM}, \tag{B.6}$$

while the expectation value of the square of these operators emerges as

$$\langle J^2_\alpha\rangle = \sum_{M=-J}^{J}\sum_{n_1=0}^{\infty}\sum_{n_2=0}^{\infty}\left[\epsilon_\alpha Re\rho^{n_1n_1n_2n_2}_{MM+2}(t)\lambda^+_{JM}\lambda^+_{JM+1} + \frac{1}{4}\rho^{n_1n_1n_2n_2}_{MM}(t)[(\lambda^-_{JM})^2 + (\lambda^+_{JM})^2]\right], \tag{B.7}$$

where $\alpha = x, y$ and $\epsilon_x = -\epsilon_y = 1/2$.

It is seen that on the two-dimensional Bloch sphere (S^2) and from the proper definition of the rotation operator [Eq. (6)] in angular momentum space, the arbitrary angular momentum components (J_n, J_k) transform as

$$\begin{pmatrix} J_n \\ J_k \end{pmatrix} = \begin{pmatrix} \sin\phi & -\cos\phi \\ \cos\phi & \sin\phi \end{pmatrix}\begin{pmatrix} J_x \\ J_y \end{pmatrix}. \tag{B.8}$$

To find the unitary transformation of $J_k \to R_{\theta,\phi}J_kR^{-1}_{\theta,\phi}$, it is observed that

$$R_{\theta,\phi}J_kR^{-1}_{\theta,\phi} \equiv e^{-i\theta\hat{J}_n}J_k, \tag{B.9}$$

where $\hat{J}_n$ is a superoperator defined by

$$\hat{J}_nJ_k = [J_n, J_k], \tag{B.10}$$

satisfying ($p \geq 0$)

$$(\hat{J}^{2p}_n - \hat{1})J_k = 0, \tag{B.11}$$

and

$$(\hat{J}^{2p+1}_nJ_k - i\hat{1}J_z) = 0. \tag{B.12}$$

Expanding the rhs of Eq. (B.9) and using

$$\hat{J}^k_nJ_k = \overbrace{[J_n,[J_n,[J_n,\ldots,[J_n,J_k]\ldots]]]}^{k\text{ stacked commutators}}, \tag{B.13}$$

the lhs of (B.9) can be written as

$$R_{\theta,\phi}J_kR^{-1}_{\theta,\phi} = J_k\cos\theta + J_z\sin\theta. \tag{B.14}$$

Analogously, it is found that powers of J_n applied to J_z satisfy the superoperator equations ($p \geq 0$)

$$(\hat{J}^{2p}_n - \hat{1})J_z = 0, \tag{B.15}$$

and

$$\hat{J}^{2p+1}_nJ_z + i\hat{1}J_k = 0, \tag{B.16}$$

which upon expansion lead to

$$R_{\theta,\phi}J_zR_{\theta,\phi}^{-1} = J_z\cos\theta - J_k\sin\theta. \tag{B.17}$$

From the inverse transformation of (B.8), it follows that the J_+ and J_- operators can be expressed in terms of J_k and J_n as

$$\begin{pmatrix} J_+ \\ J_- \end{pmatrix} = \begin{pmatrix} (J_k - iJ_n)e^{i\phi} \\ (J_k + iJ_n)e^{-i\phi} \end{pmatrix}, \tag{B.18}$$

and after some further algebra the associated rotated counterparts emerge as

$$\begin{pmatrix} R_{\theta,\phi}J_+R_{\theta\phi}^{-1} \\ R_{\theta,\phi}J_-R_{\theta,\phi}^{-1} \end{pmatrix} = \begin{pmatrix} e^{i\phi}\left(J_+e^{-i\phi}\cos^2\dfrac{\theta}{2} - J_-e^{i\phi}\sin^2\dfrac{\theta}{2} + J_z\sin\theta\right) \\ e^{-i\phi}\left(J_-e^{i\phi}\cos^2\dfrac{\theta}{2} - J_+e^{-i\phi}\sin^2\dfrac{\theta}{2} + J_z\sin\theta\right) \end{pmatrix}. \tag{B.19}$$

From Eq. (B.17) and expressing J_k in terms of J_+ and J_- through

$$J_k = \frac{1}{2}(J_+e^{-i\phi} + J_-e^{i\phi}), \tag{B.20}$$

obtained from Eq. (B.18), it follows that the transformation equation of J_z becomes

$$R_{\theta,\phi}J_zR_{\theta,\phi}^{-1} = J_z\cos\theta - (J_+e^{-i\phi} + J_-e^{i\phi})\sin\frac{\theta}{2}\cos\frac{\theta}{2}. \tag{B.21}$$

From Eq. (59) and expressing J_x and J_y in terms of J_+ and J_- through (B.18) it follows that the expectation values of J_χ, J_ξ, and J_ζ are given by

$$\begin{pmatrix} \langle J_\chi\rangle \\ \langle J_\xi\rangle \\ \langle J_\zeta\rangle \end{pmatrix} = \begin{pmatrix} \displaystyle\sum_{n_1=0}^{\infty}\sum_{n_2=0}^{\infty}\sum_{M=-J}^{J} Re\, G^-_{n_1n_2M}(\theta,\phi;t)\lambda^+_{JM} + \cos\phi\sin\theta\langle J_z\rangle \\ \displaystyle\sum_{n_1=0}^{\infty}\sum_{n_2=0}^{\infty}\sum_{M=-J}^{J} Im\, G^+_{n_1n_2M}(\theta,\phi;t)\lambda^+_{JM} + \sin\phi\sin\theta\langle J_z\rangle \\ \displaystyle -\sum_{n_1=0}^{\infty}\sum_{n_2=0}^{\infty}\sum_{M=-J}^{J} Re\, G_{n_1n_2M}(\theta,\phi;t)\lambda^+_{JM} + \langle J_z\rangle\cos\theta \end{pmatrix}, \tag{B.22}$$

where

$$G^{\pm}_{n_1n_2M}(\theta,\phi;t) = F_\pm(\theta,\phi)\rho^{n_1n_1n_2n_2}_{MM+1}(t), \tag{B.23}$$

$$G_{n_1n_2M}(\theta;\phi;t) = e^{-i\phi}\rho^{n_1n_1n_2n_2}_{MM+1}(t)\sin\theta, \tag{B.24}$$

with $F_\pm(\theta,\phi)$ given by

$$F_\pm(\theta,\phi) = \cos^2\frac{\theta}{2} \pm e^{-2i\phi}\sin^2\frac{\theta}{2}. \tag{B.25}$$

Squaring the expressions of J_χ and J_ξ and observing that

$$\langle J_z^2\rangle = \sum_{n_1=0}^{\infty}\sum_{n_2=0}^{\infty}\sum_{M=-J}^{J} M^2\rho^{n_1n_1n_2n_2}_{MM}(t), \tag{B.26}$$

along with the anticommutator

$$\langle [J_+, J_z]_+\rangle = \sum_{n_1=0}^{\infty}\sum_{n_2=0}^{\infty}\sum_{M=-J}^{J}(2M+1)\rho^{n_1n_1n_2n_2}_{MM+1}(t)\lambda^+_{JM}, \tag{B.27}$$

in conjunction with matrix elements of $\langle J_+^2\rangle$ and $\langle J_-^2\rangle$ given by Eqs. (B.1) and (B.2) and after some further algebra, it follows that the expectation values of J_χ^2 and J_ξ^2 are given by

$$\begin{aligned}\langle J_\chi^2\rangle \;=\; & \sum_{n_1=0}^{\infty}\sum_{n_2=0}^{\infty}\sum_{M=-J}^{J}\left\{\frac{1}{2}Re[F_-^2(\theta,\phi)\rho_{MM+2}^{n_1n_1n_2n_2}(t)]\lambda_{JM}^+\lambda_{JM+1}^+\right.\\ & +\frac{1}{4}\rho_{MM}^{n_1n_1n_2n_2}(t)|F_-(\theta,\phi)|^2[(\lambda_{JM}^-)^2+(\lambda_{JM}^+)^2]+M^2\rho_{MM+1}^{n_1n_1n_2n_2}(t)\cos^2\phi\sin^2\theta\\ & \left.+(2M+1)Re[F_-(\theta,\phi)\rho_{MM+1}^{n_1n_1n_2n_2}(t)]\lambda_{JM}^+\cos\phi\sin\theta\right\},\end{aligned} \tag{B.28}$$

$$\begin{aligned}\langle J_\xi^2\rangle \;=\; & \sum_{n_1=0}^{\infty}\sum_{n_2=0}^{\infty}\sum_{M=-J}^{J}\left\{-\frac{1}{2}Re[F_+^2(\theta,\phi)\rho_{MM+2}^{n_1n_1n_2n_2}(t)]\lambda_{JM}^+\lambda_{JM+1}^+\right.\\ & +\frac{1}{4}\rho_{MM}^{n_1n_1n_2n_2}(t)|F_+(\theta,\phi)|^2[(\lambda_{JM}^-)^2+(\lambda_{JM}^+)^2]+M^2\rho_{MM+1}^{n_1n_1n_2n_2}(t)\sin^2\phi\sin^2\theta\\ & \left.+\;(2M+1)Im[F_+(\theta,\phi)\rho_{MM+1}^{n_1n_1n_2n_2}(t)]\lambda_{JM}^+\sin\phi\sin\theta\right\}.\end{aligned} \tag{B.29}$$

This completes the derivation of the necessary equations to compute second-order statistical moments for the different angular momentum components involved in Eq. (62).

References

[1] R.H. Dicke, Phys. Rev. 93 (1954) 99–110.
[2] M.J. Hartmann, F.G.S.L. Brandão, M.B. Plenio, Nat. Phys. 2 (2006) 849–855.
[3] A.D. Greentree, C. Tahan, J.H. Cole, L.C.L. Hollenberg, Nat. Phys. 2 (2006) 856–861.
[4] B.J. Smith, P. Mahou, O. Cohen, J.S. Lundeen, L.A. Walmsley, Opt. Exp. 17 (2009) 23589–23602.
[5] A.M. Zagoskin, S. Ashhab, J.R. Johansson, F. Nori, Phys. Rev. Lett. 97 (2006) 077001 (4 pages).
[6] M. Scheibner, M. Yakes, A.S. Bracker, I.V. Ponomarev, M.F. Doty, C.S. Hellberg, L.J. Whitman, T.L. Reinecke, D. Gammon, Nat. Phys. 4 (2008) 291–295.
[7] R.R. Puri, Mathematical Methods of Quantum Optics, Springer, Berlin, 2001, pp. 215– 237.
[8] G. Ramon, C. Brif, A. Mann, Phys. Rev. A 58 (1998) 2506–2517.
[9] C. Emary, T. Brandes, Phys. Rev. A 69 (2004) 053804 (7 pages).
[10] C.F. Lee, N.F. Johnson, Phys. Rev. Lett. 93 (2004) 083001 (4 pages).
[11] Y. Li, Z.D. Wang, C.P. Sun, Phys. Rev. A 74 (2006) 023815 (5 pages).
[12] D. Tolkunov, D. Solenov, Phys. Rev. B 75 (2007) 024402 (7 pages).
[13] G. Chen, Z. Chen, J. Liang, Phys. Rev. A 76 (2007) 045801 (4 pages).
[14] G. Chen, X. Wang, J.-Q. Liang, Z.D. Wang, Phys. Rev. A 78 (2008) 023634 (5 pages).
[15] D. Nagy, G. Konya, G. Szirmai, P. Domokos, Phys. Rev. Lett. 104 (2010) 130401 (4 pages).
[16] H. Goto, K. Ichimura, Phys. Rev. A 77 (2008) 053811 (5 pages).
[17] O. Tsyplyatyev, D. Loss, Phys. Rev. A 80 (2009) 023803 (6 pages).
[18] M.A. Alcalde, R. Kullock, N.F. Svaiter, J. Math. Phys. 50 (2009) 013511 (17 pages).
[19] J. Larson, M. Lewenstein, New J. Phys. 11 (2009) 063027 (18 pages).
[20] S. Schneider, G.J. Milburn, Phys. Rev. A 65 (2002) 042107 (5 pages).
[21] C. Emary, T. Brandes, Phys. Rev. E 67 (2003) 066203 (22 pages).
[22] X.-W. Hou, B. Hu, Phys. Rev. A 69 (2004) 042110 (6 pages).
[23] V. Bužek, M. Orzag, M. Rosko, Phys. Rev. Lett. 94 (2005) 163601 (4 pages).
[24] N.B. Narozhny, J.J. Sánchez-Mondragón, J.H. Eberly, Phys. Rev. A 23 (1981) 236–247.
[25] M.C. Arnesen, S. Bose, V. Vedral, Phys. Rev. Lett. 87 (2001) 017901 (4 pages).
[26] T. Yu, J.H. Eberly, Phys. Rev. Lett. 93 (2004) 140404 (4 pages).
[27] R. Tanaś, Z. Ficek, J. Opt. B: Quantum Semiclass. Opt. 6 (2004) S610–S617.
[28] L. Song, X. Wang, D. Yan, Z.G. Zong, Int. J. Theor. Phys. 47 (2008) 2635–2644.
[29] K. Härkönen, F. Plastina, S. Maniscalco, Phys. Rev. A 80 (2009) 033841 (15 pages).
[30] R. Loudon, P.L. Knight, J. Mod. Opt. 34 (1987) 709–759.
[31] H.J. Kimble, Nature (London) 453 (2008) 1023–1030.
[32] C. Pérez-Campos, J.R. González-Alonso, O. Castaños, Ann. Phys. 325 (2010) 325–344.
[33] S.S. Hassan, N. Nayak, R.N. Deb, Phys. Lett. A 373 (2009) 3697–3700.
[34] R.N. Deb, N. Nayak, B. Dutta-Roy, Eur. Phys. J. D 33 (2005) 149–155.
[35] N. Nagak, R.N. Deb, B. Dutta-Roy, J. Opt. B 7 (2005) S761–S764.
[36] H. Grinberg, J. Phys. Chem. B 112 (2008) 16140–16157.
[37] H. Grinberg, Int. J. Mod. Phys. B 22 (2008) 599–633.
[38] F.T. Arecchi, E. Courtens, R. Gilmore, H. Thomas, Phys. Rev. A 6 (1972) 2211–2236.

[39] S.M. Barnett, P.M. Radmore, Methods in Theoretical Quantum Optics, Oxford Science Publications, Clarendon Press, Oxford, 1997, pp. 236–239.
[40] J.-S. Zhang, J.-B. Xu, Can. J. Phys. 87 (2009) 1031–1036.
[41] M. Kitagawa, M. Ueda, Phys. Rev. A 47 (1993) 5138–5143.
[42] H. Grinberg, Int. J. Mod. Phys. B 24 (2010) 1079–1092.
[43] J.R. Kukliński, J.L. Madajczyk, Phys. Rev. A 37 (1988) 3175–3178.
[44] C.W. Woods, J. Gea-Banacloche, J. Mod. Opt. 40 (1993) 2361–2379.
[45] M. Butler, P.D. Drummond, Opt. Acta 33 (1986) 1–5.
[46] S.M. Chumakov, J. Kozierowski, Quantum Semiclassic. Opt. 8 (1996) 775–803.
[47] H. Grinberg, Phys. Lett. A 344 (2005) 170–183.
[48] C.C. Gerry, J.H. Eberly, Phys. Rev. A 42 (1990) 6805–6815.
[49] The linear entropy is obtained by approximating $\ln \rho$ in the von Neumann entropy, with the first order term $(\rho - 1)$ in the Mercator series: $-Tr(\rho \ln \rho) \to -Tr(\rho(\rho - 1)) = Tr(\rho - \rho^2) = 1 - Tr(\rho^2) = S_L$, where the unit trace property of the density matrix has been invoked to get the second to last equality.
[50] C.H. Bennett, H.J. Bernstein, S. Popescu, B. Schumacher, Phys. Rev. A 53 (1996) 2046–2052.
[51] H. Grinberg, Phys. Lett. A 374 (2010) 1481–1487.